Supplementary Information

New Insights into Influences of Initial Oxidization States on Dynamic Reconstruction of Cu Catalysts and C−C Coupling in CO_2 Reduction

Chen Qin,[1] Xuheng Li,[1] Haoyang Li,[1] Ting Wang,[1] Xue Zhang,[1] Yuyao Wang,[1] Fuping Pan,[1,2,*] Kai-Jie Chen[1,*]

[1] School of Chemistry and Chemical Engineering, Northwestern Polytechnical University, Xi'an, Shaanxi 710072, China

[2] Chongqing Innovation Center, Northwestern Polytechnical University, Chongqing, 401135, China

* Corresponding authors emails: fupingpan@nwpu.edu.cn; ckjiscon@nwpu.edu.cn

Chemicals

Copper (II) sulfate pentahydrate ($CuSO_4 \cdot 5H_2O$, AR), hydrazine hydrate aqueous solution ($N_2H_4 \cdot H_2O$, 85.0% of volume fraction), and potassium hydrogen carbonate ($KHCO_3$, AR) were purchased from Sinopharm Chemical Reagent Co., Ltd (Shanghai, China). Polyvinyl pyrrolidone (PVP, MW=55000, AR) and Nafion (5 wt%) were purchased from Macklin. Dimethyl sulfoxide and deuterium water were purchased from Rhawn. All chemicals were used as received without further purification.

Catalysts Preparation

Synthesis of Cu_2O. 300 mg of PVP was added into 30 mL of 0.01 M $CuSO_4$ aqueous solution under magnetic stirring (300 rpm). The mixture was kept stirring for several minutes until the powders were completely dissolved. $N_2H_4 \cdot H_2O$ solution (10 μL) was then introduced into the mixture solution, forming the orange colloidal suspension of Cu_2O particles immediately. Thereafter, the resulting colloidal solution was further stirred (300 rpm) for 0.5 h for Ostwald ripening, resulting in the formation of the Cu_2O single-layer nanoshells. Finally, the nanoshells were centrifuged, washed with deionized water and ethanol, and dried overnight in a vacuum oven at 60 °C to yield Cu_2O.

Synthesis of Cu and CuO. The Cu catalyst was prepared by annealing as-prepared Cu_2O at 230 °C for 2 h under H_2/Ar (10 mol.% H_2) atmosphere. The CuO catalyst was prepared by annealing as-prepared Cu_2O at 300 °C for 5 h in air.

All catalysts were stored in the Ar-filled glove box before use.

Catalysts Characterization

The morphology, structure, and composition of catalysts were characterized by scanning electron microscopy (SEM, FEI Verios G4), transmission electron microscopy (TEM, FEI Talos F200X), high-angle annular dark-field scanning transmission electron microscopy (HAADF-STEM, FEI Themis Z), X-ray diffraction (XRD, MiniFlex), and X-ray photoelectron spectroscopy (XPS, Kratos AXIS Ultra DLD). *In-situ* Raman spectra were collected on a Horiba LabRAM HR Evolution spectroscopy at the excitation wavelength of 633 nm using a catalyst-coated gas diffusion layer as the working electrode. The contact angle was measured by a contact angle meter (Dong Guan Precise Test).

Electrochemical Measurements

All electrochemical measurements were conducted on an electrochemical workstation (Gamry Interface 1000E). To prepare the cathode electrode, a mixture that contains 5 mg of catalysts, 2 mL of isopropanol, and 50 μL of Nafion ionomer solution (5 wt% in isopropanol) was first sonicated for 60 min to obtain a catalyst ink. Then, 2 mL of the catalyst ink was sprayed onto a gas diffusion layer to achieve a catalyst loading of ~0.8 mg cm^{-2}. Electrochemical tests were conducted in an electrochemical flow cell which includes a gas chamber, a cathodic chamber, and an anodic chamber. A 0.5 M $KHCO_3$ solution was used as the anolyte and catholyte, and a proton exchange membrane (Nafion N115) was used to separate the anodic and cathodic chambers. A piece of nickel foam was used as the counter electrode, and a saturated Ag/AgCl was used as the reference electrode. The high-purity CO_2 (99.999%, 24 sccm) was introduced on the back side of the gas diffusion layer, and the electrolyte flowed in both cathodic and anodic chambers with a flow rate of 2 mL min^{-1}. The EIS measurement was carried out in the 0.5 M $KHCO_3$ solution with an amplitude of 5 mV of 10^{-1} to 10^{6} Hz. The electrochemical active surface areas (ECSAs) were determined by measuring double-layer capacitance (C_{dl}). C_{dl} was determined by measuring the capacitive current associated with double-layer charging

from the scan-rate dependence of cyclic voltammogram (CV). All potentials were converted to the reversible hydrogen electrode by E (RHE) = E (Ag/AgCl) + 0.197 V + 0.0591 V × pH without iR compensation.

Product Analysis

The gaseous products were monitored by an online gas chromatograph (GC, GC9790PLUS) equipped with a thermal conductivity detector (TCD) and a flame ionization detector (FID). The liquid products in cathode chambers were collected after electrolysis and analyzed by ^{1}H nuclear magnetic resonance (NMR, Bruker AV400) using DMSO as the internal standard and D_2O as a proton signal source.

The Faraday efficiency (FE) of gas products was calculated by the following equation:

$$FE\% = \frac{I}{I_{total}} = \frac{zFnV}{I_{total}} \times 100$$

Where I is the partial current density of a specific product.

I total is the total current density collected in the bulk electrolysis at an applied potential.

z is the number of electrons involved in the formation of a specific product. F is the Faraday constant, 96485 C mol^{-1}. n is the mole fraction of the product. V is the gas volumetric flow rate of gas.

The FE of the liquid products was calculated as:

$$FE = z \cdot F \cdot \frac{n}{Q}$$

Where z is the number of electrons transferred per mole of gas product, F is Faraday constant (96500 C mol^{-1}), n is the total amount of the liquid products determined from NMR (mole), Q is the total amount of charge passed through the cathode (A·s).

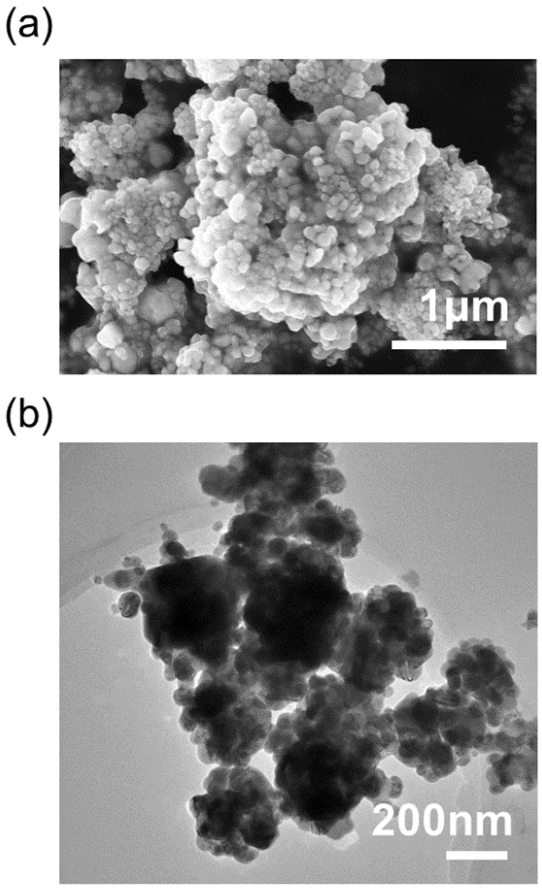

Figure S1. (a) SEM and (b) TEM images of the fresh Cu catalyst.

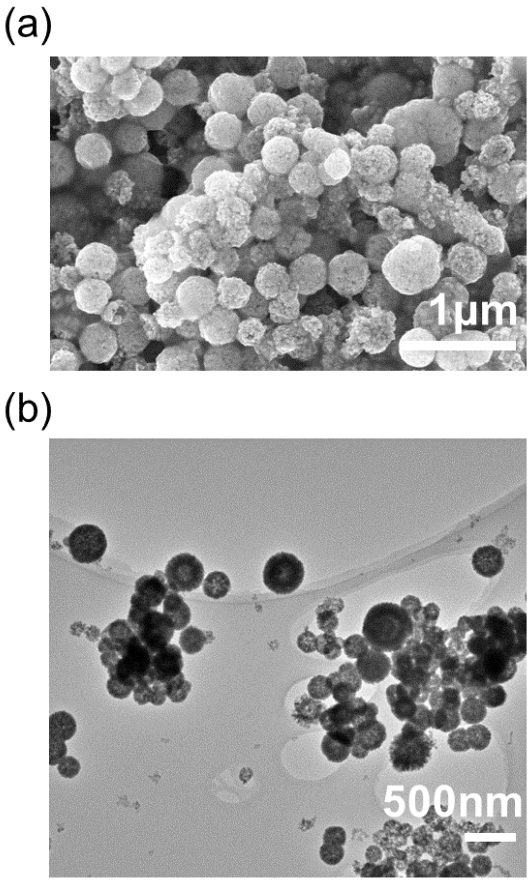

Figure S2. (a) SEM and (b) TEM images of the fresh Cu_2O catalyst.

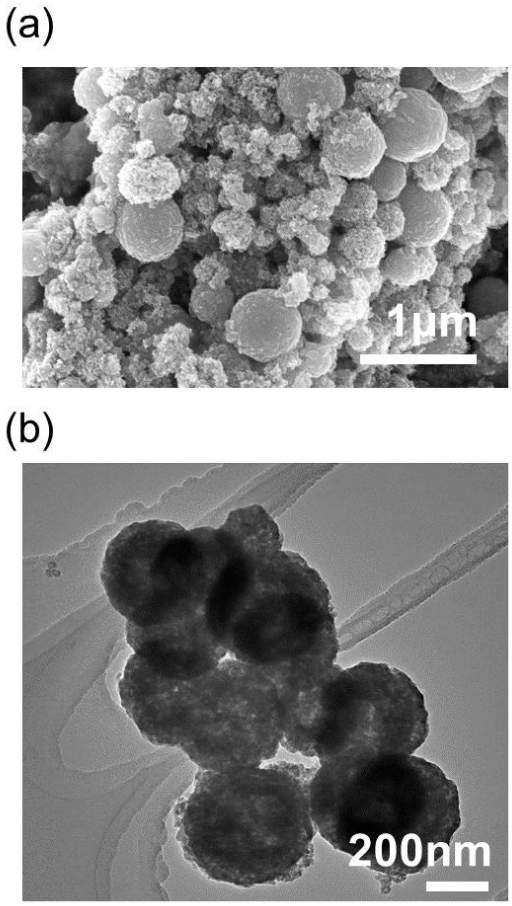

Figure S3. (a) SEM and (b) TEM images of the fresh CuO catalyst.

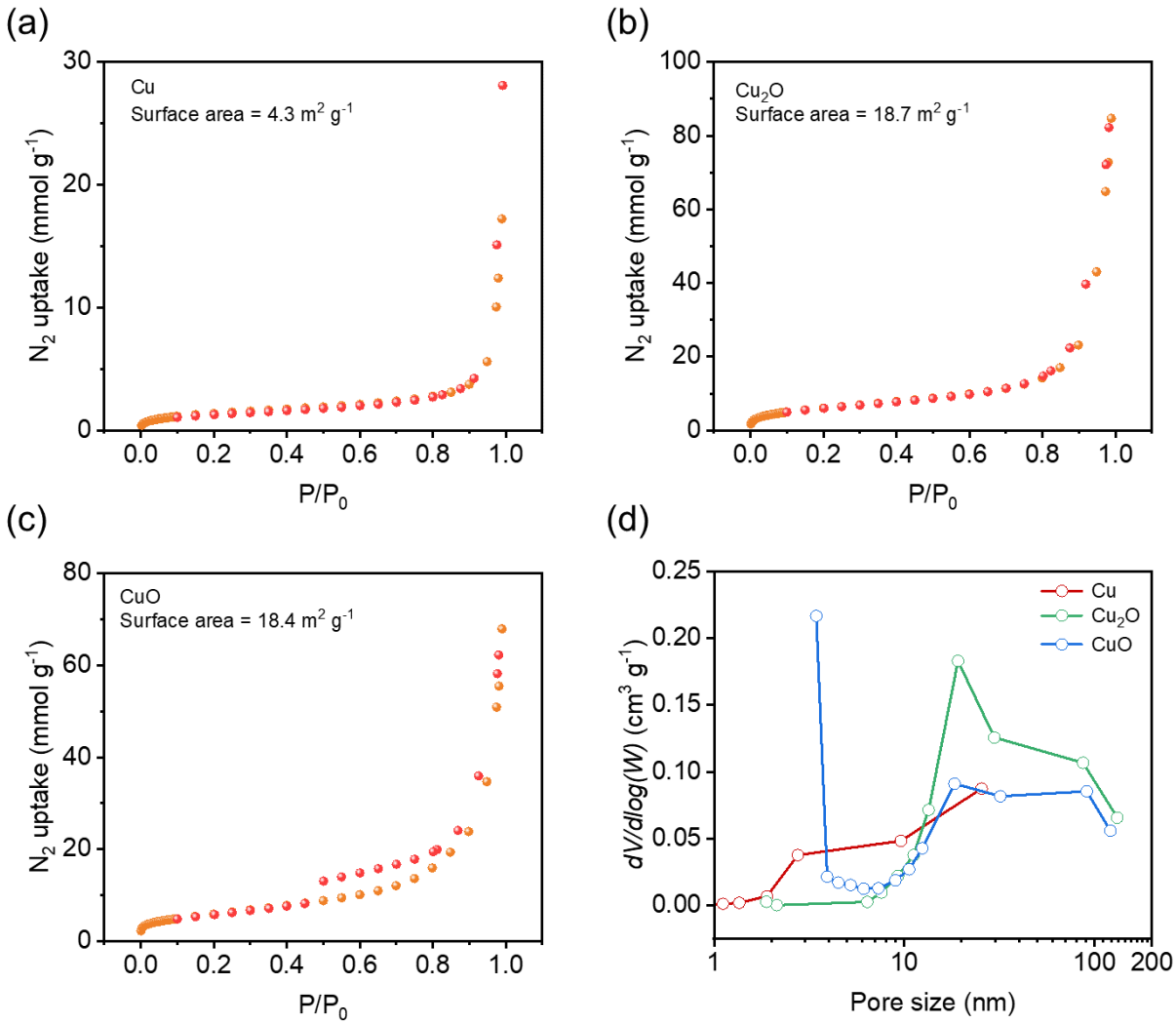

Figure S4. 77 K N_2 adsorption-desorption isotherms of Cu (a), Cu_2O (b), CuO (c). (d) Pore size distribution of Cu, Cu_2O, CuO.

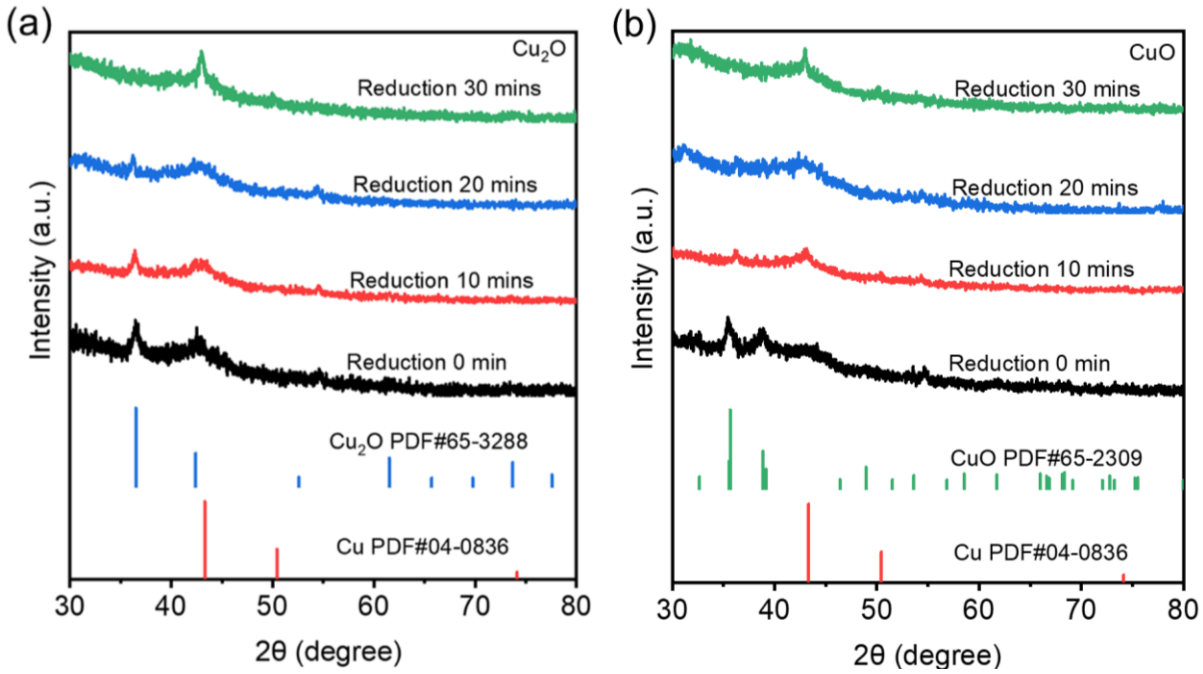

Figure S5. Time-dependent XRD patterns of Cu_2O and CuO reduced at −1.4 V vs. RHE.

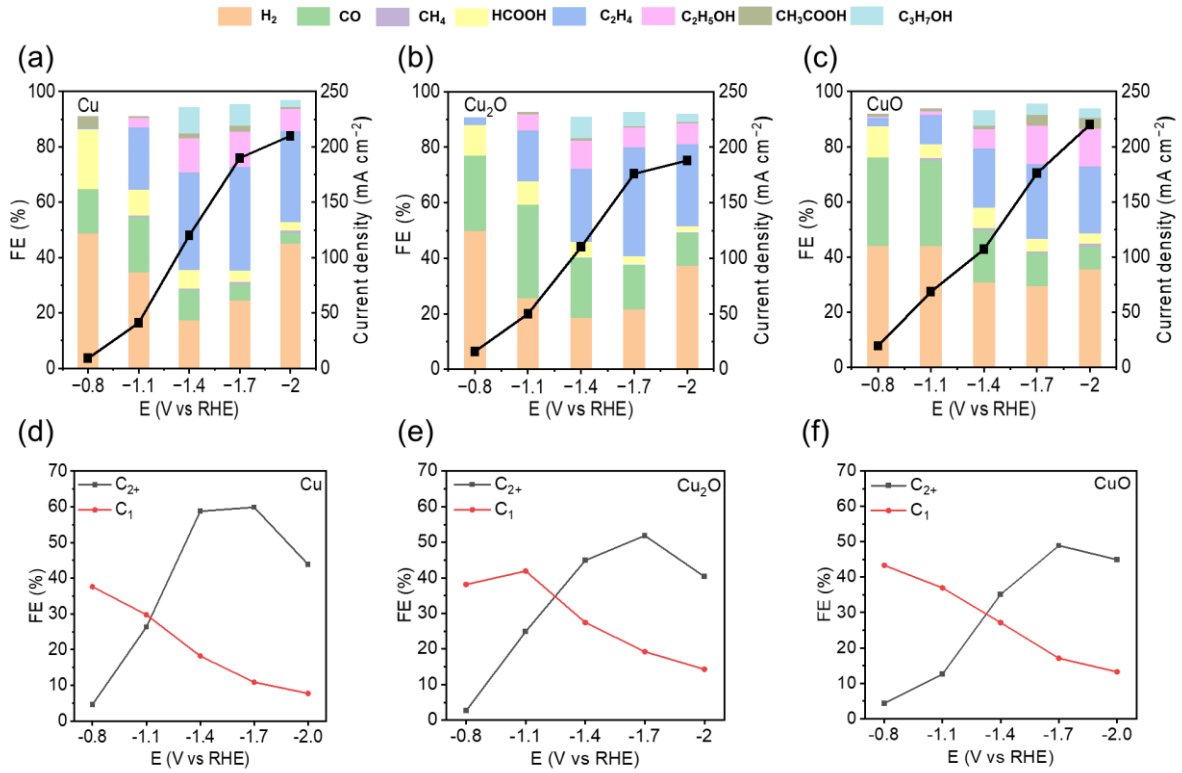

Figure S6. (a-c) FEs and current densities of CO_2RR products on the Cu, Cu_2O, and CuO catalysts. (d-f) FEs of C_{2+} and C_1 products on the Cu, Cu_2O, and CuO catalysts.

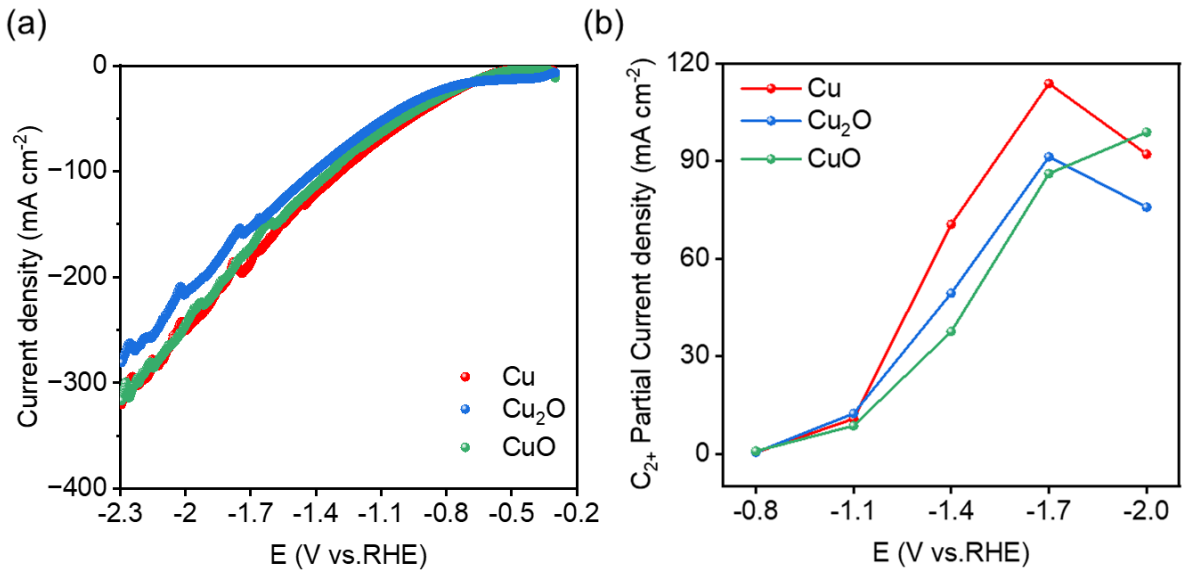

Figure S7. (a) Linear sweep voltammetry (LSV) curves and (b) C_{2+} partial current density of for various catalysts.

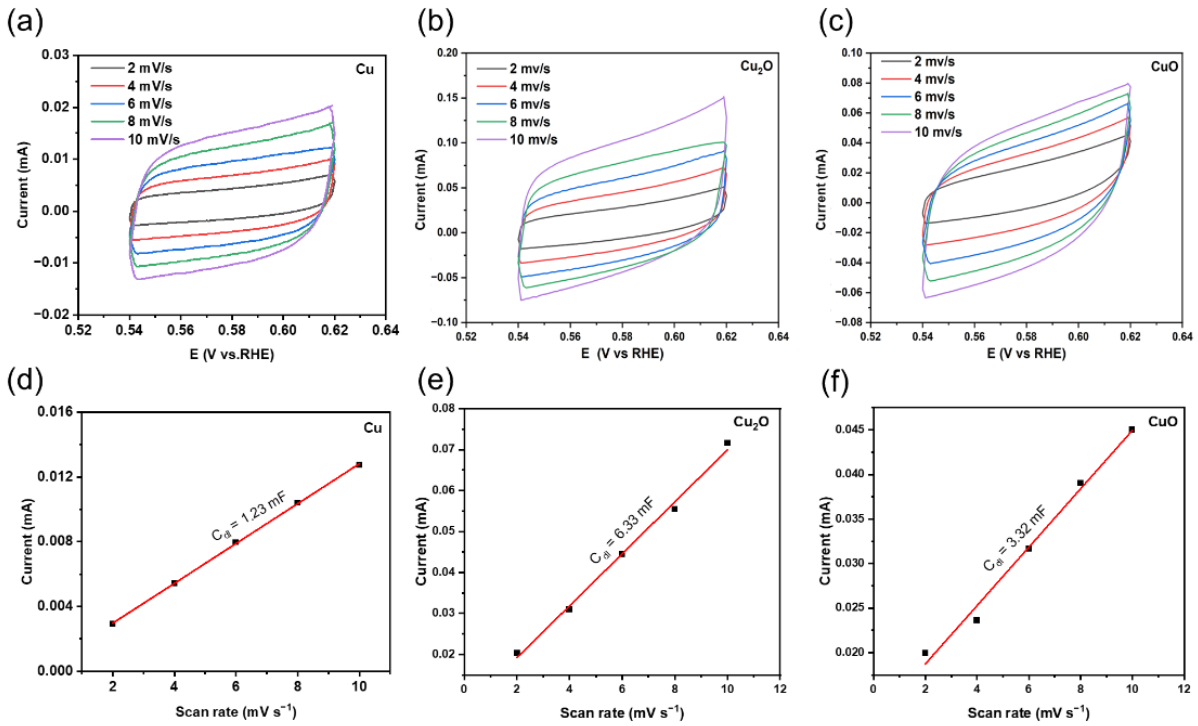

Figure S8. (a-c) Cyclic voltammogram curves of Cu (a), Cu_2O (b), and CuO (c) at various scan rates (2, 4, 6, 8, and 10 mV s^{-1}). (d-f) Capacitive currents against scan rates at 0.60 V to obtain the double-layer capacities (C_{dl}, mF $cm^{-2}_{(electrode)}$) based on the slopes of these plots for Cu (d), Cu_2O (e), and CuO (f).

Electrochemically active surface area (ECSA, cm^2) was estimated as:

$$ECSA = \frac{C_{dl}}{C_{gc}}$$

where C_{gc} is the double layer capacitance (mF cm^{-2}) of the glassy carbon electrode surface, for which the typical value of 0.029 mF cm^{-2} was used.

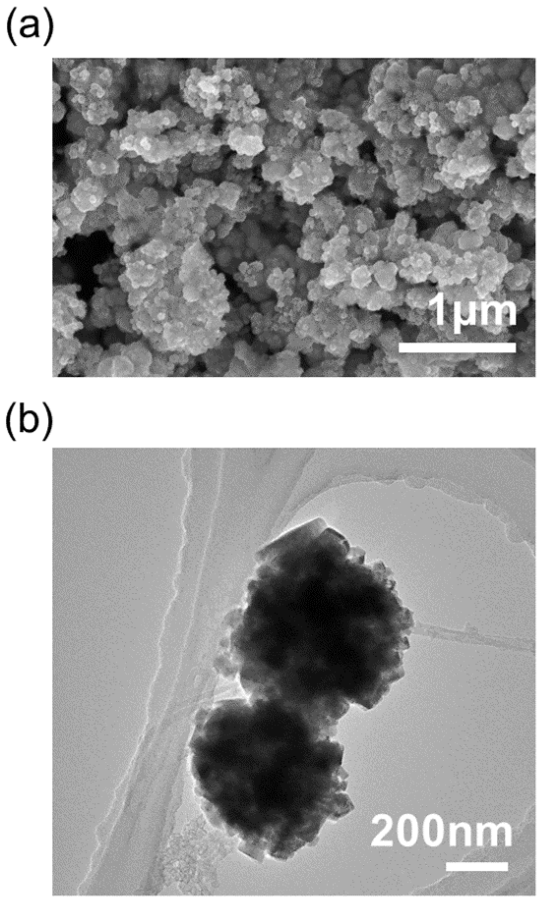

Figure S9. (a) SEM and (b) TEM images of the Cu catalyst after CO_2 reduction.

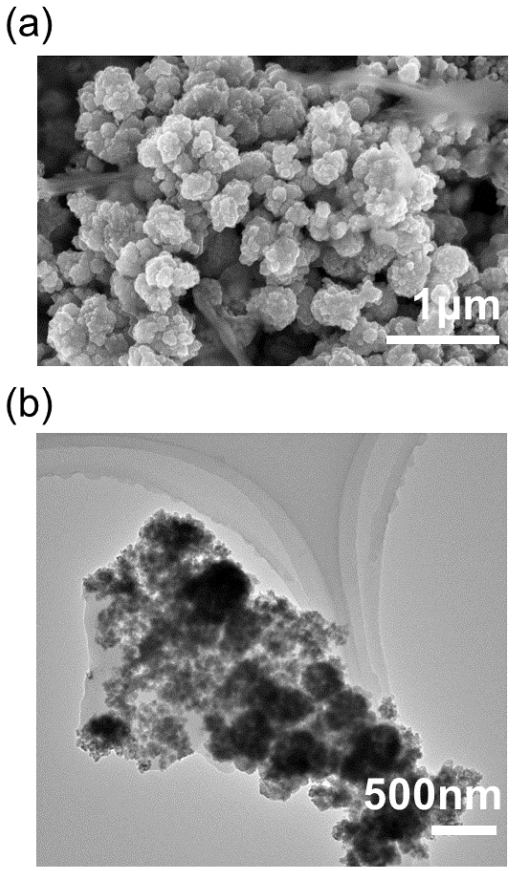

Figure S10. (a) SEM and (b) TEM images of the Cu_2O catalyst after CO_2 reduction.

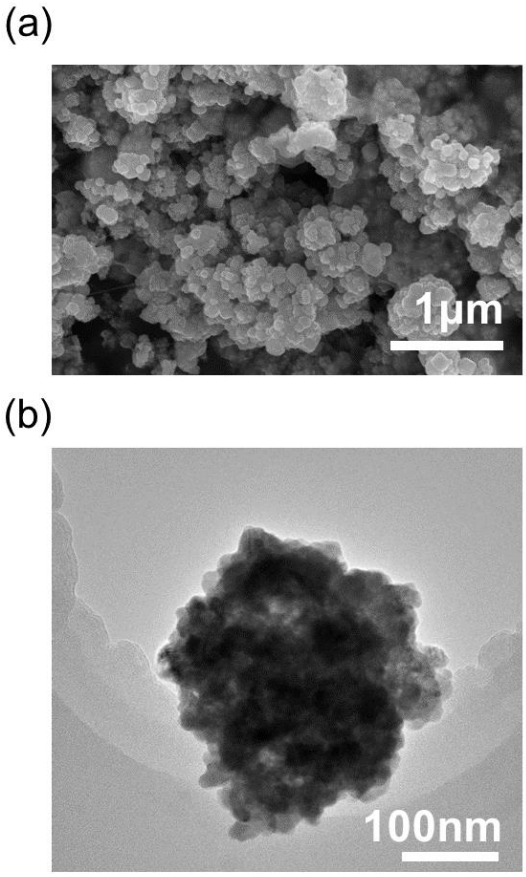

Figure S11. (a) SEM and (b) TEM images of the CuO catalyst after CO_2 reduction.

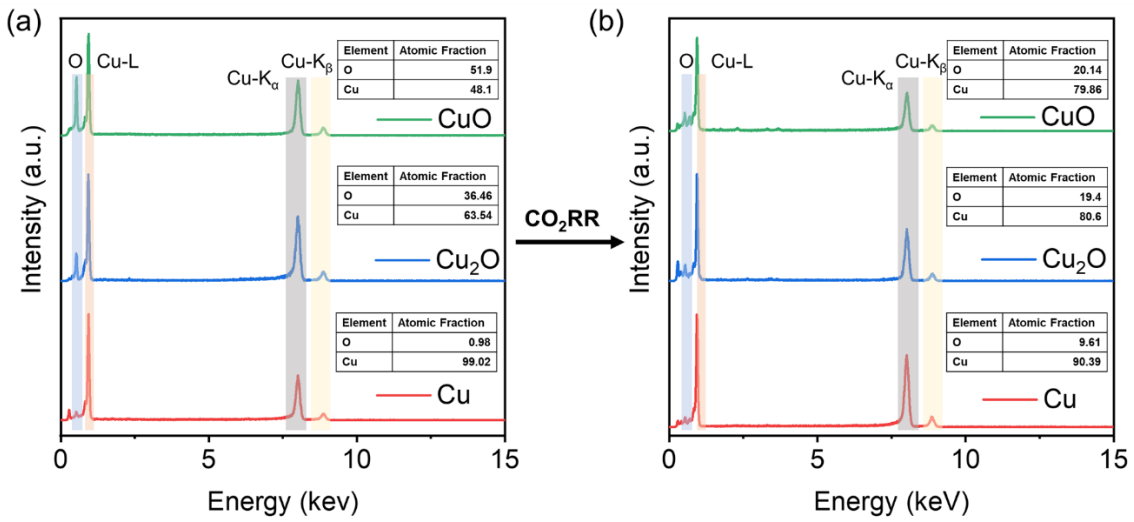

Figure S12. (a, b) EDS spectra for catalysts before (a) and after CO_2RR (b).

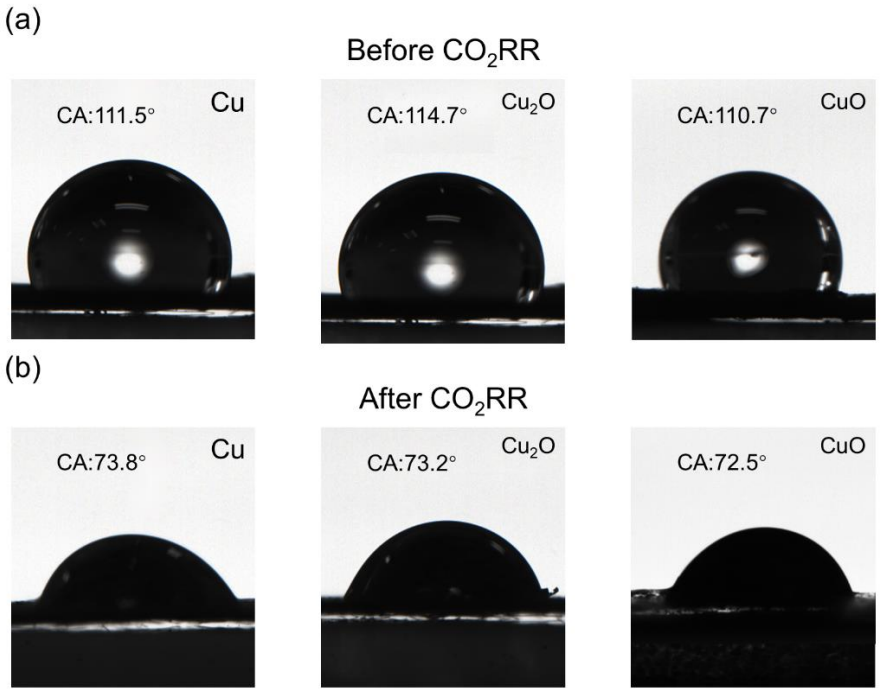

Figure S13. Contact angles of 0.5 M $KHCO_3$ on GDL-loaded Cu, Cu_2O, and CuO catalysts before (a) and after CO_2RR (b).